

Numerical simulations of local shock reformation and ion acceleration in supernova remnants

R. E. Lee¹, S. C. Chapman^{2,1} and R. O. Dendy^{3,1}

¹*Department of Physics, University of Warwick, Coventry CV4 7AL, UK*

²*Radcliffe Institute for Advanced Study, Harvard University, USA*

³*UKAEA Culham Division, Culham Science Centre, Abingdon, OX14 3DB, UK*

1 Introduction

Protons form the majority constituent of Galactic cosmic rays, however the mechanism for their initial acceleration remains an outstanding problem in astrophysics. Supernova remnants (SNRs) provide the most likely source of kinetic energy to sustain the cosmic ray population, and it is widely accepted that ions are accelerated at these sites. Until recently a firm observational link between supernova remnants and locally accelerated ions has been lacking, however X-ray and γ -ray spectra from supernova remnant RX J1713.7-3946 (see, for example, Ref. [1]) can only be explained by accelerated ions. Several mechanisms are postulated to accelerate particles at SNR shocks. Fermi acceleration [2], which arises as a particle repeatedly scatters off turbulent structures on either side of the shock, is in principle capable of accelerating ions to these high energies [3]. This however requires an initially supra-thermal ion population. Identifying pre-acceleration mechanisms that can energise initially non-relativistic ions constitutes the ‘injection’ problem. To portray the full dynamically reforming SNR shock structure and associated ion acceleration, it is desirable to retain the full electron kinetics (see Refs. [4, 5]). Here we present results of high resolution particle-in-cell (PIC) code simulations, for parameters relevant to SNR shocks. These show that the time-dependent electromagnetic fields at the reforming shock can accelerate ions from background to supra-thermal energies, thus providing a natural mechanism for ion injection.

2 Shock reformation

The key phenomenology in our PIC simulations arises from the non-timestationary nature of the reforming shock. This is shown in Fig. 1, which plots magnetic field strength as a function of x and time. As with all Figures in this work, this is presented in a frame where the downstream plasma is at rest, using data collected from a time segment of the simulation when the shock has formed and is propagating independently of the boundary conditions. Units are normalized to ion upstream parameters, thus λ_{ci} and ω_{ci} are the upstream ion cyclotron radius and frequency, and \mathcal{E}_{inj} is the ion injection energy. The shock moves upstream, from right to left of the simulation box, with peaks in mag-

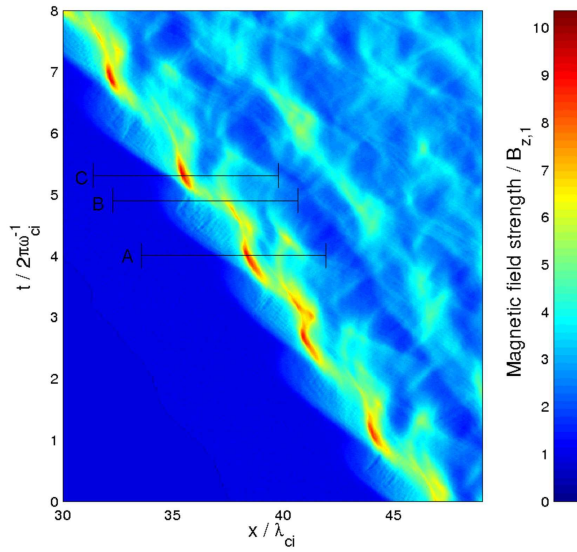


Figure 1: Evolution of perpendicular magnetic field strength, over time (vertical axis), and space (horizontal axis), showing the non-timstationary reformation on local ion cyclotron spatio-temporal scales. The shock speed ranges from 0 to $3\langle u_s \rangle$, where $\langle u_s \rangle$ is the average shock speed derived from the Rankine-Hugoniot conditions. The differing stages of a reformation cycle can be seen in Figs. 2, 3 and 4, which show simulation snapshots at spatio-temporal coordinates labelled A, B and C respectively.

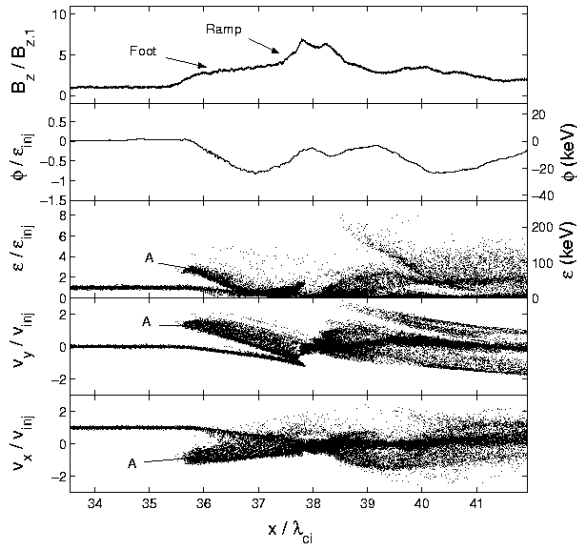


Figure 2: Spatial cross section of the simulation in the shock region at $t = 4.0\omega_{ci}$, corresponding to line A in Figure 1. The top panel (panel 1) shows perpendicular magnetic field, normalized to the upstream value $B_{z,1}$. Panel 2 shows the potential in units normalized to the ion injection energy (\mathcal{E}_{inj}) on the left hand side, and in keV on the right. Panel 3 shows the kinetic energy of the ions normalized to \mathcal{E}_{inj} and keV. Panel 4 shows the ion velocity in the y direction (perpendicular both to the shock normal and the magnetic field) normalized to injection velocity (v_{inj}). Panel 5 shows ion phase space (x versus v_x) with velocities normalized to v_{inj} . The feature A in the three lower frames relates to foot formation by shock-reflected ions.

netic field (the shock ramp) recurring on the time scale of the local ion cyclotron period. Over the course of each cycle, a stationary shock ramp forms at the turnaround point of protons in the foot region. Then a new foot region extends into the upstream region as protons reflect from this new shock front (“A” in Fig 2). A new ramp (magnetic field peak) then starts to form at the upstream edge of this foot region as the reflected ions start to gyrate back to the shock front (“B” in Fig 3), and another cycle begins. The last of the original foot region ions gyrate into the downstream plasma (“B” in Fig 4), while the new shock starts to reflect a new foot region population (“A” in Fig 4). The shock thus propagates upstream (left) in a stepwise fashion.

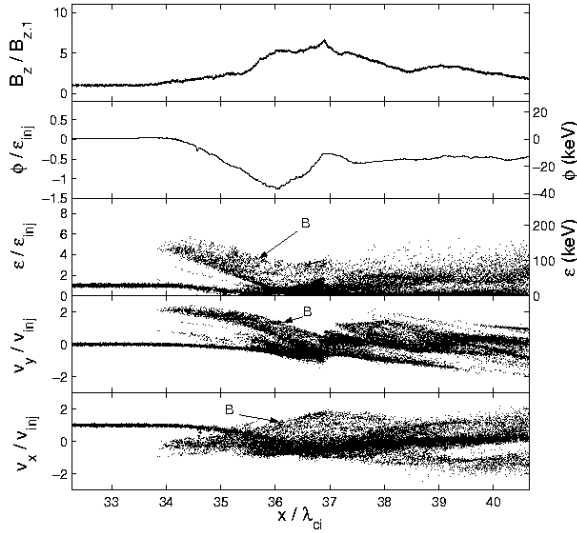


Figure 3: Spatial cross section of the simulation in the shock region at $t = 4.9\omega_{ci}$, corresponding to line B in Figure 1. The axes are as in Figure 2. The feature B in the three lower frames relates to energised reflected ions whose Larmor orbits carry them back towards the shock.

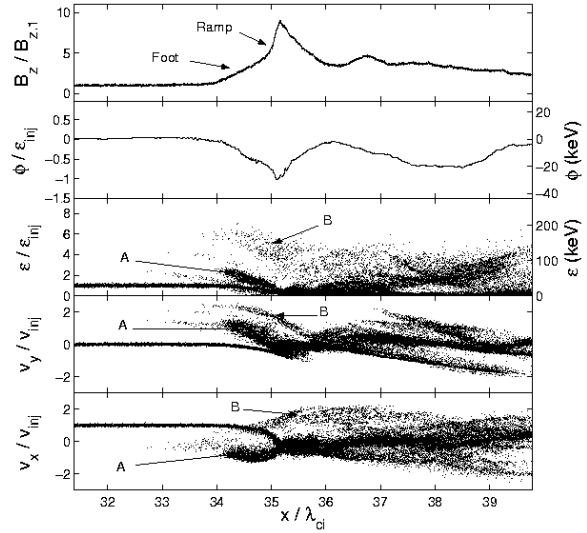


Figure 4: Spatial cross section of the simulation in the reformed shock region at $t = 5.3\omega_{ci}$, corresponding to line C in Figure 1. The axes are as in Figure 2. Both reflected ions reforming the foot (A), and energised ions passing through the shock (B), are visible.

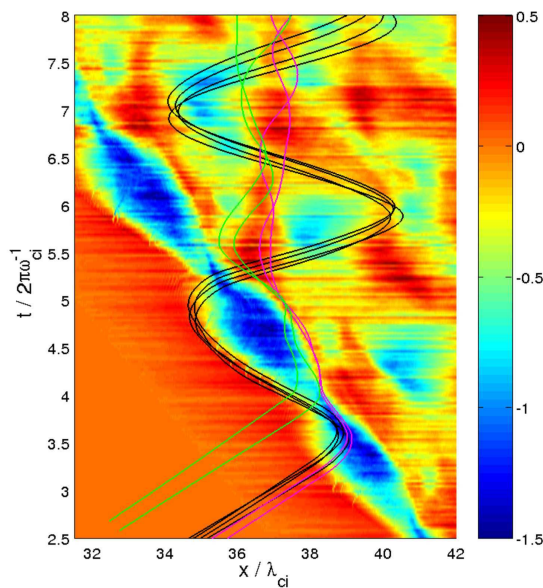


Figure 5: Potential ϕ/\mathcal{E}_{inj} (values in colour bar) over time (vertical axis) and space (horizontal axis), with trajectories for: sample ions that eventually gain energy $\sim 6 \times \mathcal{E}_{inj}$ (black); and ions that remain at low energies, and interact with the shock before (purple), or after (green), those ions that go to high energy. The variation of ϕ on both the electron and ion spatio-temporal scales is visible, with electron phase space holes (or equivalently ion acoustic caviton structures) occurring on electron scales (and previously associated with electron acceleration, see, for example, Refs. [6, 7]), forming along the leading edge of the bulk potential well that varies on ion spatio-temporal scales, and whose extent is defined by the high energy ions.

3 Ion acceleration

A proportion of inflow ions are specularly reflected at the shock ramp, when it is stationary in the downstream rest frame, so that $v_x \rightarrow -v_x$ (“A” in Figs. 2 and 4). These are then accelerated in the foot region via a gain in velocity perpendicular to both the shock normal and magnetic field. Reflected ions define the shape and extent of the foot region, with those reflected earliest in the cycle travelling furthest upstream and reaching the highest energies $\sim 6\mathcal{E}_{inj}$. The energy gain scales linearly with the ion mass and the square of the inflow speed.

4 Conclusions

Treating the full kinetic problem of a supercritical quasi-perpendicular collisionless shock, including the dissipation as given by electron kinetics, we find the foot-ramp-overshoot structure obtained by earlier hybrid code simulations that yield time-stationary shocks. However the structure in our PIC simulations is fundamentally time-dependent: for the parameters of interest here, no time-stationary shock solutions exist, and instead we observe cyclic reformation on ion cyclotron time scales. As a consequence, the shock generates a suprathermal population of ions at energies up to $6\mathcal{E}_{inj}$. These energies scale linearly with the mass ratio, and with the square of the inflow velocity; this is because the spatio-temporal scales of the electromagnetic fields responsible for the energisation are determined by the kinetics of the injected ions: $L = v_{inj}/\omega_{ci}$, $T = 1/\omega_{ci}$. The ion acceleration mechanism is governed by the low frequency bulk $\phi(t)$ of the foot’s potential well; we refer to Ref. [5] for further discussion of the key elements. The scaling of our PIC results to realistic parameters from astrophysical observation, suggests that accelerated ions would leave the SNR shock foot region with energies of order 10 – 20 MeV. However the simulation phenomenology has been tested over only a small parameter range.

Acknowledgements: This work was supported in part by UK PPARC and EPSRC.

References

- [1] R. Enomoto et al. *Nature*, 416:823–826, April 2002.
- [2] E. Fermi. *Physical Review*, 75:1169–1174, 1949.
- [3] A.R. Bell. *Mon.Not.R.Astron.Soc.*, 182:147–156, 1978.
- [4] M. Scholer, I. Shinohara, and S. Matsukiyo. *JGR*, 108(A1):SSH4–1, 2003.
- [5] R.E. Lee, S.C. Chapman, and R.O. Dendy. *Astrophys.J.*, 604:187–195, 2004.
- [6] M.E. Dieckmann, K.G. McClements, S.C. Chapman, R.O. Dendy, and L.O’C. Drury. *Astron.Astrophys.*, 356:377–388, 2000.
- [7] H. Schmitz, S. C. Chapman, and R. O. Dendy. *Astrophys.J.*, 570:637–646, 2002.